Atmospheric
Chemistry
and Physics

# Emission factors of $SO_2$, $NO_x$ and particles from ships in Neva Bay from ground-based and helicopter-borne measurements and AIS-based modeling

**J. Beecken**[1], **J. Mellqvist**[1], **K. Salo**[1], **J. Ekholm**[1], **J.-P. Jalkanen**[2], **L. Johansson**[2], **V. Litvinenko**[3], **K. Volodin**[3], and **D. A. Frank-Kamenetsky**[4]

[1]Chalmers University of Technology, Earth and Space Sciences, Gothenburg, Sweden
[2]Finnish Meteorological Institute, Helsinki, Finland
[3]State Geological Unitary Company Mineral, St. Petersburg, Russia
[4]Committee for Nature Use, Environmental Protection and Ecological Safety, St. Petersburg, Russia

*Correspondence to:* J. Beecken (beecken@chalmers.se)

**Abstract.** Emission factors of $SO_2$, $NO_x$ and size-distributed particle numbers were measured for approximately 300 different ships in the Gulf of Finland and Neva Bay area during two campaigns in August/September 2011 and June/July 2012. The measurements were carried out from a harbor vessel and from an Mi-8 helicopter downwind of passing ships. Other measurements were carried out from shore sites near the island of Kronstadt and along the Neva River in the urban area of Saint Petersburg. Most ships were running at reduced speed (10 kn), i.e., not at their optimal load. Vessels for domestic and international shipping were monitored. It was seen that the distribution of the $SO_2$ emission factors is bi-modal, with averages of 4.6 and 18.2 $g_{SO_2}$ $kg_{fuel}^{-1}$ for the lower and the higher mode, respectively. The emission factors show compliance with the 1 % fuel sulfur content Sulfur Emission Control Areas (SECA) limit for 90 % of the vessels in 2011 and 97 % in 2012. The distribution of the $NO_x$ emission factor is mono-modal, with an average of 58 $g_{NO_x}$ $kg_{fuel}^{-1}$. The corresponding emission related to the generated power yields an average of 12.1 $g_{NO_x}$ $kWh^{-1}$. The distribution of the emission factors for particulate number shows that nearly 90 % of all particles in the 5.6 nm to 10 μm size range were below 70 nm in diameter. The distribution of the corresponding emission factors for the mass indicates two separated main modes, one for particles between 30 and 300 nm and the other for above 2 μm. The average particle emission factors were found to be in the range from 0.7 to $2.7 \times 10^{16}$ particles $kg_{fuel}^{-1}$ and 0.2 to 3.4 $g_{PM}$ $kg_{fuel}^{-1}$, respectively. The $NO_x$ and particulate emissions are comparable with other studies. The measured emission factors were compared, for individual ships, to modeled ones using the Ship Traffic Emission Assessment Model (STEAM) of the Finnish Meteorological Institute. A reasonably good agreement for gaseous sulfur and nitrogen emissions can be seen for ships in international traffic, but significant deviations are found for inland vessels. Regarding particulate mass, the values of the modeled data are about 2–3 times higher than the measured results, which probably reflects the assumptions made in the modeled fuel sulfur content. The sulfur contents in the fuel retrieved from the measurements were lower than the previously used assumptions by the City of Saint Petersburg when carrying out atmospheric modeling, and using these measurements it was possible to better assess the impact of shipping on air quality.

## 1 Introduction

Shipping is a major means of transport. In 2012, about 9 billion tons of goods were transported by ships, corresponding to almost 80 % of the worldwide merchandise trade by volume, with about 4 % growth as compared to 2011 (UNCTAD, 2013). As much as shipping is important as a means of transport it is also a source for air pollution. In earlier stud-

ies, it is estimated that about 15 % of the anthropogenic $NO_x$ emissions and 7 % of the $SO_2$ emissions are due to shipping. Of these emissions around 70 % occur within 400 km from land (Corbett et al., 1999). Gaseous and particle emissions from ships have significant impacts on nature, climate and human health. Corbett et al. (2007) estimated the number of humans dying prematurely due to emissions from ships to be 60 000 each year.

The significance of air pollution by ships has been acknowledged by policy makers on the global level. Under the umbrella of the International Maritime Organization (IMO) international limits have been agreed upon with the aim to reduce the emissions of $SO_x$ and $NO_x$ as agreed in the MARPOL Annex VI protocol. As a consequence, a global cap of 3.5 % fuel sulfur content, by mass, has been in effect since 2012. This cap is intended to be reduced to 0.5 % in 2020. However, there are stronger limits set for Sulfur Emission Control Areas (SECA), like the North Sea and the Baltic Sea. Here ships are not allowed to bunker fuel with more than 1 % sulfur content since 2010, which was further reduced to 0.1 % in January 2015.

For marine diesel engines, there are different regulations for the emission of $NO_x$ depending on the ships' construction dates. The caps defined under Tier 1 are valid for ships with engines built between the years 2000 and 2010. These caps are reduced in Tier 2 by 20 % for ships with engines built after 2011 and a further reduction of 80 % in Tier 3 is intended for ships with engines built in the year 2016 and afterwards. For Tier 3, there will be exceptions for smaller recreational vessels and certain countries.

The coming requirements for low fuel sulfur content in the SECA areas will be rather costly for the shipping industry, which has a strong concern, together with policy makers, that the new rules will not be obeyed. It is therefore suggested that the regulations are enforced by compliance monitoring to promote a level playing field within the shipping industry. Within the Swedish project Identification of Gross-Polluting Ships (IGPS) (Mellqvist and Berg, 2010; Beecken et al., 2014) a monitoring system has been developed for measuring gaseous and particulate emissions of individual ships within harbor areas and on the open sea, with the capability to check compliance with the new emission rules in the SECA areas.

Within the context above, measurements of ship emission factors were carried out for various air pollutants during two campaigns in the Neva Bay area and the Gulf of Finland in 2011 and 2012, respectively, as part of the IGPS-project and the EU project BSR-Innoship.

A new system for measuring ship emissions which was previously used on airborne platforms (Beecken et al., 2014) was applied for the first time for measurements from ground and boat. In this study, the particulate measurements were extended to an upper particle size of 10 μm, instead of 500 nm, and a more precise total number counter was used. A considerable fraction of the ships measured in this study correspond to river barges and other ships running only in the eastern part of the Gulf of Finland and the Neva River, complementing the earlier study which corresponded primarily to ocean-going ships, such as containers vessels, oil tankers and ferry boats. The measurements in 2011 were carried out at the transition period when Russia ratified the Annex VI protocol in April 2011 requiring maximum 1 % sulfur content in the fuel which came into effect on 8 July 2011 (AMSA, 2014). Since very few real world emission measurements of ships have been conducted worldwide, especially in the eastern Baltic where to our knowledge no such studies have been carried out before, there is a need for this type of data to be able to model ship emissions more accurately and subsequently carry out air quality modeling. The data derived in this study are compared to the STEAM model (Jalkanen et al., 2009, 2012; Jalkanen and Johansson, 2013), which is widely used, e.g., within the HELCOM (Baltic Marine Environment Protection Commission - Helsinki Commission) community to model individual ship emissions and to estimate emissions on regional and global scale. The objective of this study was to help to readjust and refine this model and to demonstrate the performance of such a model.

## 2   Methods

The results presented in this paper were obtained using an extended system for the identification of gross-polluting ships (IGPS), (Mellqvist and Berg, 2010). A short overview on the instrumentation is given in Sect. 2.1. The system's main components are described in detail by Beecken et al. (2014). Additional components are an optical particle sizer for particles up to 10 μm and a condensation particle counter.

### 2.1   Instrumentation

$CO_2$ was measured with cavity ring-down spectroscopy (CRDS) (O'Keefe and Deacon, 1988) using a modified flight Picarro G2301-m greenhouse gas monitor with a response time, $t_{90}$, of less than 1 s, the time that is needed at a step change to reach 90 % of the final value. The instrument produces a $CO_2$, $H_2O$ and $CH_4$ value once every second which is obtained by sequentially measuring the three species for around 0.3 s per species.

For determining the sulfur emission factor in the form of $SO_2$, a modified Thermo 43iTLE trace gas monitor was used. An internal UV flash lamp stimulates fluorescence of the $SO_2$ which is proportional to its volume mixing ratio (VMR) (Luke, 1997). The instrument is custom-modified through the elimination of a "hydrocarbon kicker", and larger pump speed yielding a response time, $t_{90}$, of about 2 s to allow flow rates for the detection of short and distinct plumes. The $SO_2$ instrument is cross-sensitive to NO, with a $SO_2$ VMR reading corresponding to 1.5 % of the VMR of NO. The removal of the kicker, which is simply a Teflon tube coil, also makes the

instrument cross sensitive to aromatic volatile organic compounds (VOC) with about 1 % of the VOC VMR, but in most cases, ships emit very little VOC (Williams et al., 2009), so this is only a problem when measuring in proximity to large VOC sources, such as refineries, since this may cause fluctuating background readings.

The emission factor of $NO_x$ was obtained with a custom modified Thermo 42TL trace gas monitor. A larger pump is used to obtain lower instrument pressures, and a modification in the software allows for the user to externally control whether NO, $NO_x$ or the zero background should be measured, instead of continuously switching between measurement and zero background. The VMR of NO is determined by a chemiluminescent reaction of NO with ozone. The intensity of the light emitted is proportional to the VMR of NO (Kley and McFarland, 1980). The instrument uses a catalytic converter that converts the $NO_2$ to NO, so the sum of NO and $NO_2$ ($NO_x$) is obtained. The instrument has a response time, $t_{90}$, of 1 s.

An instrument based on electric mobility, the Engine Exhaust Particle Sizer (EEPS, TSI 3090), was applied to analyze the number size distribution in the range from 5.6 to 560 nm in 32 size channels. The particles in a stream of sampled air are charged by a corona and then forced to move in an electrical field which deflects them towards a column of electrodes (Johnson et al., 2004). The EEPS is originally intended for fast particle sizing of engine exhaust, and due to its fast simultaneous sampling at 10 Hz and response time, $t_{90}$, of 0.5 s it also was found to be suitable for measurements of particulate ship emissions (Hallquist et al., 2013; Jonsson et al., 2011), even from aircraft (Beecken et al., 2014).

The size distribution of bigger particles was measured with an Optical Particle Sizer (OPS, TSI 3330). The OPS measures the backscattered intensity of light pulses onto a stream of sample air with particles. The number and size of the particles is determined from the detected backscattered light flashes. The diameter of the detected particles ranges from 0.3 to 10 µm and is binned into 16 size channels. The instruments response time, $t_{90}$, is 2 s.

The total number of particles was determined with TSI 3787 General Purpose Water-Based Condensation Particle Counter (CPC) (Hering et al., 2005). Sampled particles are grown in a supersaturated chamber and afterwards optically counted. This CPC measures particles bigger than 5 nm up to approximately 1 µm with a response time, $t_{90}$, of less than 0.3 s. The CPC was only used during the 2012 campaign.

## 2.2 Calculation of emission factors

The calculation of emission factors is similar for gas and particle data. The evaluation of sampled plumes is illustrated in Fig. 1. After the identification of a plume, a baseline is determined and subtracted from the in-plume values. The background-corrected data, given in mixing ratios units (here in ppb or ppm), is integrated over the plume for each sub-
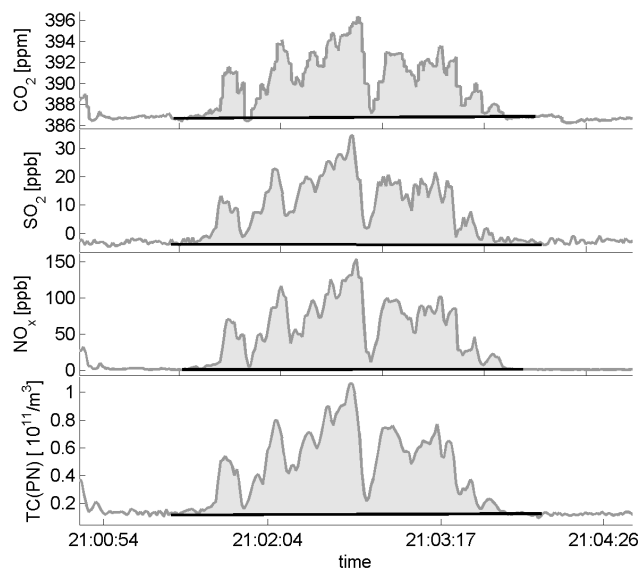


**Figure 1.** Example of plume evaluation on a typical plume, here from the Ro-Ro (Roll-on/roll-off) cargo ship *Pauline Russ*. The signal of three gas channels and one particle channel are shown as a grey line. The black line is the found background baseline to be subtracted from the plume. The plume's signal is integrated over time (grey shaded area). The ratio of the areas of $SO_2$ and $NO_x$ to $CO_2$ is used for further calculation of the emission factors.

stituent $X$, and then normalized against the integrated $CO_2$ values according to Eq. (1). Furthermore, the calculated ratio is converted to a mass-based emission factor, i.e., mass of pollutant versus mass of fuel, by scaling with the molecular weights of the species $X$ and fuel; the latter obtained as molecular weight of carbon corrected with the assumed carbon content of the fuel, i.e., 87 %. Note that for the calculation of fuel sulfur content the species $X$ is replaced with pure sulfur, e.g., $20\,g_{SO_2}\,kg_{fuel}^{-1}$ corresponds to a fuel sulfur content (FSC) of 1 %. In the case of $NO_x$, its molecular weight is assumed to correspond to $NO_2$, following the IMO technical code MEPC.177(58) (MEPC, 2008).

It is common to compare the performance of different engines, especially for $NO_x$, by using load-based emission factors, i.e., mass of pollutant versus generated crank shaft power. In order to obtain this value (specific emission factor) the mass-based emission factors is multiplied with the brake-specific fuel consumption (BSFC), which relates the consumed fuel to the generated power. This number, which varies between $160–250\,g_{fuel}\,kWh^{-1}$ depending on ship type, was in this study obtained from the STEAM model data (Jalkanen et al., 2009, 2012), which in turn is based on ship specific data from the IHS Maritime ship register (IHS Global, 2014). In the cases of no registered BSFC, a default value of $200\,g_{NO_x}\,kWh^{-1}$ was assumed.

$$\mathrm{EF}(X)_{\mathrm{g/kg_{fuel}}} = \frac{M(X)_{\mathrm{g/mol}} \times \int [X]_{\mathrm{ppb}} - [X_{\mathrm{bgd}}]_{\mathrm{ppb}} \mathrm{d}t}{\frac{M(C)_{\mathrm{g/mol}}}{0.87} \times \int [CO_2]_{\mathrm{ppm}} - [CO_{2,\mathrm{bgd}}]_{\mathrm{ppm}} \mathrm{d}t}$$

(1)

For the calculation of the particle number emission factor EF(PN) in Eq. (2), the excess number concentration per volume unit in the plumes was related to the excess mass concentration per volume unit of $CO_2$ (assuming $T_{\mathrm{avg}} = 290$ K, $p_{\mathrm{avg}} = 101\,325$ Pa) using the ideal gas law, with the ideal gas constant $R = 8.314$ J mol$^{-1}$ K$^{-1}$. The emission factor of $CO_2$ is here calculated using Eq. (1).

$$\mathrm{EF(PN)}_{\#/\mathrm{kg_{fuel}}} = \frac{\int [PN]_{\#/\mathrm{cm}^3} - [PN_{\mathrm{bgd}}]_{\#/\mathrm{cm}^3} \mathrm{d}t}{\int [CO_2]_{\mathrm{kg/cm}^3} - [CO_{2,\mathrm{bgd}}]_{\mathrm{kg/cm}^3} \mathrm{d}t}$$
$$\times \mathrm{EF(CO_2)}_{\mathrm{kg/kg_{fuel}}}$$

(2)

$$[CO_2]_{\mathrm{kg/cm}^3} = [CO_2]_{\mathrm{ppm}} \times M(CO_2)_{\mathrm{g/mol}}$$
$$\times \frac{p_{\mathrm{Pa}}}{R_{\mathrm{J(mol \times K)}} \times T_K} \times 10^{-15}$$

(3)

The calculation of the emission factor of the particle mass is done analogously to Eq. (1) by substituting particle number (PN) with particle mass (PM). A unity density of 1 g cm$^{-3}$ was arbitrarily assumed for the sake of qualitative comparison, although diesel particle density varies with composition and size between 0.5 and 1.23 g cm$^{-3}$ for particles between 50 and 150 nm (Barone et al., 2011; Virtanen et al., 2002; Petzold et al., 2008). For the estimation of the emission factor of the particle mass, the particle sized data from the EEPS and OPS instruments were used. The results for the particle sizers were additionally compensated for by the actual size dependent diffusion losses under laminar flow conditions (Hinds, 1999).

The geometric mean diameter (GMD) was calculated using Eq. (4) (Hinds, 1999). It should be noted that the EEPS measures the particle diameter $D_{\mathrm{p}}$ depending on the electromobility of the particles while the OPS measures diameters depending on the optical properties of the particles.

$$\mathrm{GMD_{nm}} = \exp\left(\frac{\sum [n_i \times \ln(D_{pi,\mathrm{nm}})]}{N}\right)$$

(4)

The symbols $n_i$ and $N$ denote the number of particles in the respective size bin and the total number of particles of all size bins, respectively. $D_{pi}$ is the center diameter of the respective size bin.

## 2.3 Calibrations

Calibrations of the gas-phase instruments were performed repeatedly during the measurement campaigns. The calibration gases were obtained from the Russian D.I. Mendeleev Institute for Metrology (VNIIM) Standard Materials Service.

In 2011, cylinders with known gas mixtures were used for $CO_2$ (401 ppm $\pm$ 3 %, 356 ppm $\pm$ 3 %) and NO (250 ppb $\pm$ 10 %). $SO_2$ was calibrated with a dynamic gas calibrator, based on mass flow controller GGS-03-03 from OOO Monitoring, that mixes a high concentrated $SO_2$ (53.4 ppm) with zero air by controlling the respective mass flow. $SO_2$ was calibrated in several steps up to 529 ppb. Because the maximum flow of the gas calibrator was less than the flow of the measurement system, the calibration gas was filled in Tedlar gas sampling bags which were subsequently used in the calibration. This procedure was only carried out twice during the campaign.

In 2012, a high-flow dynamic gas calibrator (Thermo 146i), in conjunction with a zero-air supply (Thermo 1160), was used to dilute $SO_2$ at 63.7 ppm $\pm$ 3 % and NO at 64 ppm $\pm$ 5 % in several calibration steps to volume mixing ratios between 0 and 300 ppb for both gases. For $CO_2$ two calibration mixtures of 365 ppm $\pm$ 3 % and 418 ppm $\pm$ 3 % were used. This gas calibrator eliminated the need for Tedlar bags and therefore the calibration could be done several times each measurement day.

The measurement precision of the gas-phase instruments was estimated from the standard deviation during the calibrations, over a period between 30 and 120 s. The measurement precision of the $SO_2$ instrument was recorded as 3.6 % in 2012, while for 2011 it was assumed to be 5 % due to fewer calibrations. For the NO$_x$ analyzer, the standard deviation of the response was recorded to be 0.5 % in 2011 and 1.3 % in 2012, respectively.

The plume samples were corrected using calibration factors. The uncertainty due to the interpolation of the calibration factors is estimated by evaluating the mean standard deviation between two adjacent calibration points. It was 0.2 and 0.7 % for $CO_2$ respectively for 2011 and 2012. For $SO_2$, it was 4.7 and 2.0 % and for NO, 4.0 and 2.1 % for these years.

The size response of the particle sizers was validated for both campaigns with vaporized Diethylhexyl Sebacate (DEHS) with particle diameters, $D_{\mathrm{p}}$, between 200 and 300 nm during the campaigns with good agreement.

## 2.4 Uncertainties

The results of repeatedly measured plumes from the same ship were used to estimate the precision, i.e., random uncertainty, of the emission factor measurements from the helicopter. The $1 \times \sigma$ precision values were 19.5 % for $SO_2$ and 23.7 % for NO$_x$, respectively, based on the mean precision of 12 ships that were measured at least three times.

For the ground-based measurements, the random uncertainty is expected to be smaller, since the plumes were present for a considerably longer time, and the random uncertainties above are therefore considered as an upper level.

The systematic uncertainties consist of the calibration uncertainties and the uncertainty by the model-based retrieval of the BSFC. Furthermore, other studies indicate that the sulfur content may be systematically underestimated by 1–19 % when applying ratio measurement of $SO_2$ over $CO_2$, hence assuming that all sulfur is emitted in the form of $SO_2$ (Schlager et al., 2006; Agrawal et al., 2008; Moldanová et al., 2009, 2013; Balzani Lööv et al., 2014). Since the conclusions from these studies are quite inconsistent, this potential uncertainty is not included in the error estimation here.

Following the IMO guidelines, the carbon mass fraction in fuel varies between 85 and 87.5 % (MEPC, 2005). The carbon mass fraction of heavy fuel oil is closer to the lower end and diesel oil closer to the higher end of this interval. In this study a carbon mass fraction of 87 % was assumed in the calculation of the emission factors. The maximum error due to this assumption is approximately 2.4 %.

The overall measurement uncertainty is calculated as the root of sum of squares (RSS) of the systematic and random uncertainties. Where the uncertainties of the two campaigns were combined, the higher uncertainty was taken into account. This yields the total uncertainties of 21 and 26 % for the mass-based emission factors of $SO_2$ and $NO_x$, respectively. For the calculation of the specific emission factor for $NO_x$ an additional uncertainty of 11 % for the BSFC data is added, yielding a total uncertainty of 29 %.

The uncertainties above are comparable to estimates that were done in a previous study using the same system (Beecken et al., 2014), where the uncertainties in the mass-based emission factors were 20 % for $SO_2$ and 24 % for $NO_x$. Alföldy et al. (2013) report similar uncertainties of 23 % for $SO_2$ and 26 % $NO_x$. It should be noted that the uncertainty for emission factor of $SO_2$ of 20 % was found for FSCs of around 1 %. In a study by Mellqvist et al. (2015), the emission of a ship which was known to run voluntarily on marine gas oil and hence with FSC of 0.1 % or below was repeatedly measured, yet at different occasions, using the same system at a fixed site. The measurements indicate an average FSC of 0.06 % with a standard deviation of about 0.03 %. Under the assumption that the FSC used by the ship would be the same during all measurements, this would indicate an uncertainty of about 50 % for the $EF(SO_2)$ for ships running on low FSC around 0.1 %.

According to the instrument certificate, the EEPS was analyzed by the manufacturer (TSI) against a scanning mobility particle sizer (SMPS) system for particle size distribution accuracy and a CPC (TSI CPC 3022, $D_{p,min} = 7$ nm) for total number accuracy using both 100 nm classified and polydisperse emery oil. According to the manufacturer's certificate, the deviation of particle size distribution was found to be less than 7 % and the deviation in total number less than 20 %.

Cross-comparison measurements of the EEPS were performed at our laboratory with a SMPS (TSI DMA 3081 and TSI CPC 3787) with ammonium sulfate at concentrations between $1.85 \times 10^{11}$ and $8.36 \times 10^{11}$ particles m$^{-3}$. It was found that the GMDs in a size region around 30 nm measured with the EEPS are around 14 % below those measured with the SMPS. In this study it is assumed that the CPC counts all particles. The SMPS System which was used in this comparison was validated with standardized polystyrene latex spheres (PLS) of known sizes between 70 and 500 nm. From the deviations, it was seen that the particle diameters were underestimated by the SMPS by less than 1 % at an offset of less than 7 nm. A comparison with the CPC indicated an underestimation of the total particle number of about 30 % by the EEPS. A similar discrepancy has been observed in another study (Jonsson et al., 2011), when comparing the same type of instruments.

In this study it was not possible to perform any cross validations for the OPS. Instead the manufacturer's quality assurance certificates have to be relied on for error estimation, corresponding to an uncertainty in size resolution of 3.5 % and in number better than 10 % for particles around 0.5 µm.

## 2.5 Ship emission modeling

The STEAM model generates ship specific emissions of $CO_2$, $SO_2$, $NO_x$ and particulates at the time and location of the actual ships (Jalkanen et al., 2009, 2012; Jalkanen and Johansson, 2013). The model uses as input values the position reports generated by the automatic identification system (AIS), this system is on-board every vessel that weighs more than 300 t throughout the globe. The AIS system provides automatic updates of the positions and instantaneous speeds of ships at intervals of a few seconds. The model requires as input also the detailed technical specifications of all fuel consuming systems on-board and other relevant technical details of the ships, taken from the IHS Maritime ship register (IHS Global, 2014), for all the ships.

The propelling power of each ship is predicted as a function of its speed. In STEAM, the fuel type and sulfur content for different engines are assigned on a per vessel basis and for main and auxiliary engines separately. If the sulfur content of the fuel is known explicitly, it is used by the model. In any other case the sulfur content is determined by engine properties (engine power, angular velocity and stroke type) according to the classification proposed by Kuiken (2008). The $NO_x$ emissions are modeled according to IMO three tier approach as a function of engine angular velocity (revolutions per minute; rpm). For vessels built before the year 2000, the so-called Tier 0 ships, the $NO_x$ emission factors 10 % above the Tier 1 level are assigned (Starcrest, 2012). Emission factors for PM are determined based on the FSC as described in Jalkanen et al. (2012). This approach assumes a linear relationship between sulfate aerosol formation and fuel sulfur content, but engine load level changes to sulfur–sulfate conversion efficiency were not modeled. Note that when comparing the results of modeled data with the measured data, in STEAM the gas-phase emissions of sulfur were calculated as $SO_x$, which is the sum of $SO_2$ and $SO_3$, while during the
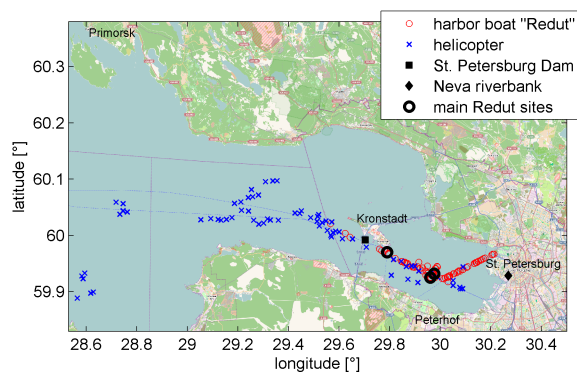
**Figure 2.** Map overview of the measurement sites. Most of the measurements from the harbor boat *Redut* were performed from the main *Redut* sites. Some during the passage between these sites and the port. (Map data© OpenStreetMap)

campaigns just $SO_2$ was measured. However, in the comparison it is assumed that the abundance of $SO_3$ is negligible.

## 3 Measurements

Measurements in the Neva Bay were conducted from land and ship while the measurements in the Gulf of Finland were carried out from a Mi-8 helicopter. The locations of the measurements are presented in Fig. 2. The measurements with the helicopter were mostly performed on ships at open sea to the west of the St. Petersburg Dam. The measurement campaigns took place in August/September 2011 and June/July 2012. Most measurements were carried out from a harbor vessel, but for 3 days in 2011, measurements were also conducted from a vehicle parked along the Neva River and at the St. Petersburg Dam. For 5 days in July 2012, measurements were carried out from a Mi-8 helicopter.

Most of the measurements were conducted onboard the work vessel *Redut*, Fig. 3, while anchoring downwind the main ship passage trail in the Neva Bay between the island of Kronstadt and Saint Petersburg. This ship passage is used by all commercial ships going to and from Saint Petersburg and by river ships that sail further up the Neva River. In 2011, these measurements took place between 22 August and 5 September, and in 2012 from 26 June to 5 July. In Neva Bay, vessel speed is restricted to 10 kn, with an exception for fast ferries running up to 30 kn, and many ships were hence running at half their design speed, with low engine loads. This impacts, in particular, the emission factors of $NO_x$ and particles (Lack et al., 2011; Cappa et al., 2014). The ships on the open sea had speeds up to 20 kn.

The sample inlets themselves were mounted to the front of the vessel at 6.5 m above sea level in 2011 and 8.5 m in 2012, far away from the smokestack at the aft.

Stationary measurements were carried out from a van on 18 and 19 August 2011, close to the storm surge gates at





**Figure 3.** Top: work vessel *Redut* with sample inlets (photo of *Redut* taken by M. Pingoud); bottom: Mi-8 helicopter with sample inlet.

the Saint Petersburg Dam. The sample inlets were mounted onto a mast at around 7 m above sea level. In addition, similar measurements were performed during the night from 20 to 21 August 2011, studying the traffic on the Bolshaya Neva river arm near the Blagoveshchensky Bridge, while the bridges were open for ship traffic. The sample inlets were 6.5 m above sea level.

Measurements from onboard the Mi-8 helicopter, Fig. 3, were conducted between 5 and 10 July 2012, with about 17 flight hours in total. In the helicopter, a probe was used that was pointed straight out, with 50 cm distance from the fuselage. To minimize the influence of downwash from the rotor, the helicopter was operated at a steady forward motion, usually between 40 and 70 kn. This minimized variations in the $CO_2$ values that were interpreted as turbulence caused by the rotor. The typical flight altitude was around 65 m above sea surface to be able to sample the ship plumes and the helicopter generally flew outside the Neva Bay, as illustrated in Fig. 2.

During the helicopter measurements, larger ships were predominantly chosen for the measurements while for the ground-based measurements, plumes of any of the passing ships were measured, since the latter were done in a passive manner.
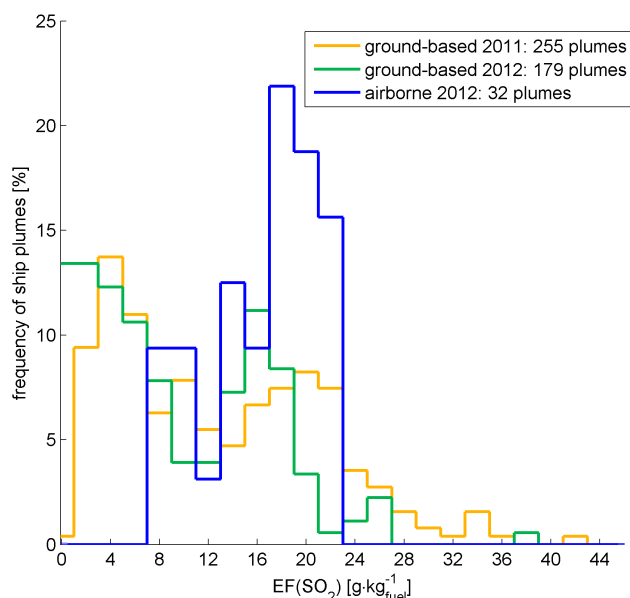
**Figure 4.** The frequency distribution of the measured emission factors of $SO_2$. Two main modes can be identified for the ground-based measurements; one for small $SO_2$ emission factors below and around $4\,\mathrm{g_{SO_2}\,kg_{fuel}^{-1}}$, and the other one for $20\,\mathrm{g_{SO_2}\,kg_{fuel}^{-1}}$ in 2011 and $16\,\mathrm{g_{SO_2}\,kg_{fuel}^{-1}}$ in 2012.

The domestic vessels are divided into cargo boats (Nevsky vessels) and tankers (Volgoneft), operating on the Neva River and the east part of the Gulf of Finland and fast hydrofoil ferries traveling between the city of St. Petersburg and Peterhof.

The measured data was compared to the modeled data using the STEAM ship emission model.

## 4 Results and discussion

In total 466 plumes from 311 different vessels were observed, of which 434 plumes were observed during the ground-based measurements and 32 plumes were observed from the helicopter. Most of the plumes which were measured from the helicopter were sampled repeatedly for the same vessel. Results from individual measurements can be found in the Supplement.

### 4.1 Sulfur dioxide

The frequency distribution of the measured $SO_2$ emission factors is shown in Fig. 4. The distributions of the ground-based measurements show that there are two prominent modes separated by the gap at $12\,\mathrm{g_{SO_2}\,kg_{fuel}^{-1}}$ with about 50 % of the measurements on either side. The median emission in the lower mode is about $4.6\,\mathrm{g_{SO_2}\,kg_{fuel}^{-1}}$ while the first and third quartiles can be found at 2.7 and $7.5\,\mathrm{g_{SO_2}\,kg_{fuel}^{-1}}$, respectively. The corresponding median in the higher mode is 18.2, and 15.4 and $21.3\,\mathrm{g_{SO_2}\,kg_{fuel}^{-1}}$ for the first and third quartiles.
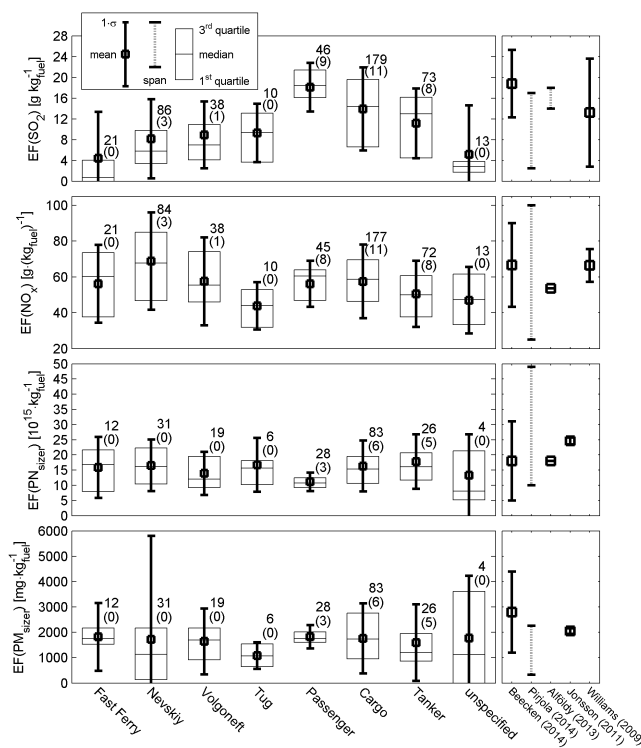


**Figure 5.** $SO_2$, $NO_x$ and particle emission factors over different ship types and comparison to results from the literature. The number close to the boxes denotes the number of sampled plumes from this ship type; numbers in brackets, the fraction of plumes that were measured from the helicopter. Ship types Nevsky, Volgoneft and Fast Ferry are shown separately from their main groups.

The distribution of the helicopter-borne measured emission factors are almost entirely located around $20\,\mathrm{g_{SO_2}\,kg_{fuel}^{-1}}$.

The emission factors of $SO_2$ for different ship types are shown in Fig. 5. Nearly all values are below $20\,\mathrm{g_{SO_2}\,kg_{fuel}^{-1}}$. However, a clear difference in the sulfur emission can be seen for the different types. Vessels which are operated mostly in domestic waters, i.e., fast ferries, Nevsky class cargo vessels, Volgoneft tankers and tugs, emitted less than $10\,\mathrm{g_{SO_2}\,kg_{fuel}^{-1}}$, indicating low fuel sulfur content, while the internationally operating ships had higher fuel sulfur contents.

The measured $SO_2$ emission factors indicate that there was a reduction of 13 % in the sulfur emission factors between 2011 and 2012, with 80 % of the plumes corresponding to emission factors below $21.2\,\mathrm{g_{SO_2}\,kg_{fuel}^{-1}}$ in 2011 and below $18.4\,\mathrm{g_{SO_2}\,kg_{fuel}^{-1}}$ in 2012. The results obtained from ground-based measurement in Neva Bay in 2011 and 2012 indicate that 90 and 97 %, respectively, of the ships complied with IMO FSC limit of 1 %, when taking the measurement uncertainty into account. The 32 ships measured outside Neva Bay from the helicopter all complied with the IMO sulfur limits.
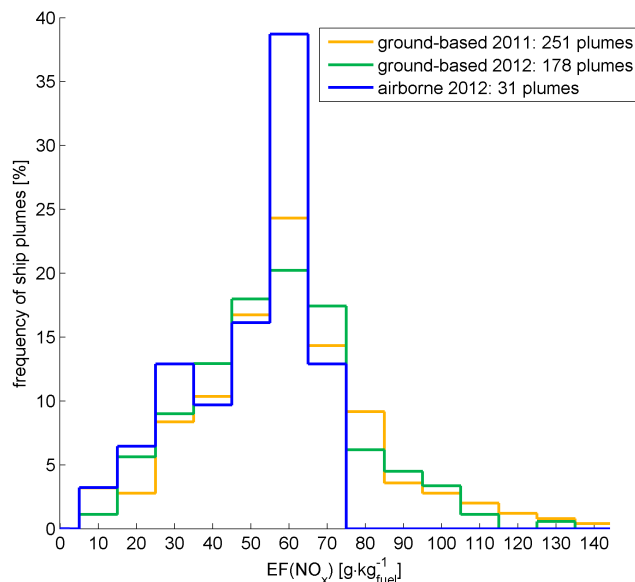
**Figure 6.** The frequency distribution of the measured emission factors of NO$_x$. It can be seen that there is a distinct peak around 60 g$_{NO_x}$ kg$_{fuel}^{-1}$ which can be seen for all campaigns. For helicopter-borne measurements, no samples were seen with NO$_x$ emission factors above 75 g$_{NO_x}$ kg$_{fuel}^{-1}$.



**Figure 7.** Averaged normalized size distribution of the EF(PN) and the cumulative sum of the median EF(PM) distribution over particle size. Around 77 % of the particles in the range 5.6 nm to 10 μm were found to be between 7 and 65 nm in size. Around 70 % of the EF(PM) is from particles below 300 nm.

## 4.2 Nitrogen oxides

In Fig. 6 it can be seen that the NO$_x$ emission factors are distributed around a single peak. The median of the NO$_x$ emission related to the amount of consumed fuel can be found at 58 g$_{NO_x}$ kg$_{fuel}^{-1}$ and the first and third quartiles at 44 and 70 g$_{NO_x}$ kg$_{fuel}^{-1}$. The measured median NO$_x$ emission factor in this study is 12 % below the average value found by Williams et al. (2009), probably due the fact that most ships were running at low speed with relatively low loads (Borkowski et al., 2011). These lower values are consistent with other studies (Alföldy et al., 2013; Pirjola et al., 2014) also taking place in harbor areas or channels where ships were running at reduced speed (Cappa et al., 2014).

For the power related emission the corresponding median is at 12.1 g$_{NO_x}$ kWh$^{-1}$ and the first and third quartiles at 9.1 and 14.4 g$_{NO_x}$ kWh$^{-1}$. The NO$_x$ emission factors are shown for different ship types in Fig. 5.

## 4.3 Particulate matter

The normalized size distributions in number, EF(PN), and mass units, EF(PM), for individual plume measurements are shown in Fig. 7. Ninety percent of the measured particles were smaller than 70 nm. It can be seen that the 10th to the 90th percentile range of the GMDs is between 24 and 53 nm. In a similar study (Jonsson et al., 2011), in the harbor of Gothenburg, Sweden, measurements were carried out from about the same distance as in this study, and in this
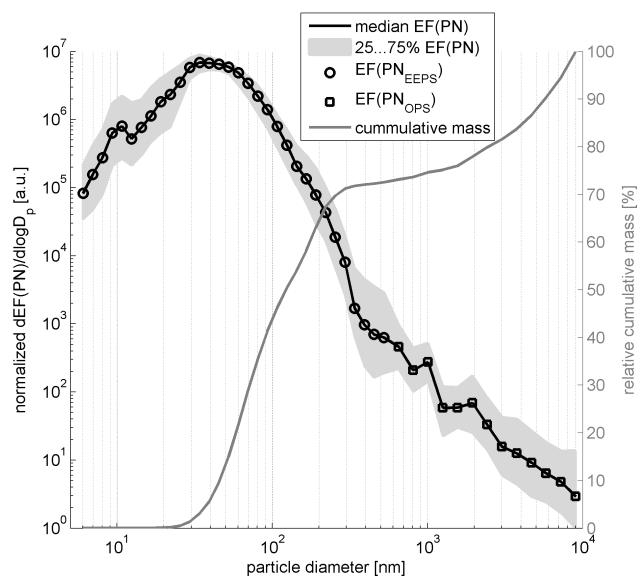
case the GMD values were between 21 and 39 nm for six selected ships, consistent with the data given in this paper. The graph showing EF(PN) also indicates the presence of a second smaller particle mode with diameters of about 10 nm, probably corresponding to fresh particles produced in the flue gas, which is also observed in other studies (Hallquist et al., 2013; Moldanová et al., 2013). Around 70 % of the total measured EF(PM) particulate mass below 10 μm consists of particles smaller than 300 nm. In the distribution of the particle mass emission factor, two separate size regions were identified to contribute to the mass, one for particles from 30 to 300 nm and the other for particles above 2 μm. This is based on the assumption that all measured particles have spherical shape and unit density.

A comparison of the total particle numbers from measurements with the CPC and the combined measurements with the EEPS and OPS shows high correlation ($R^2 = 0.98$) and a root mean square error (RMSE) of $0.17 \times 10^{16}$ particles kg$_{fuel}^{-1}$. However, the CPC results show 34 % higher values than the combined particle sizers.

In Fig. 8, the frequency distributions of the measured emission factors of total particle numbers for each instrument are presented, whereas the result for the frequency distribution for particulate mass, EF(PM), is shown in Fig. 9. The statistical distributions of the particle emission factors for number and mass are shown for the different ship types in Fig. 5.

Altogether, the number and mass emission factors measured by the particle sizers lie within the ranges of 0.7 to $2.7 \times 10^{16}$ particles kg$_{fuel}^{-1}$ and of 0.2 to 3.4 g$_{PM}$ kg$_{fuel}^{-1}$, respec-
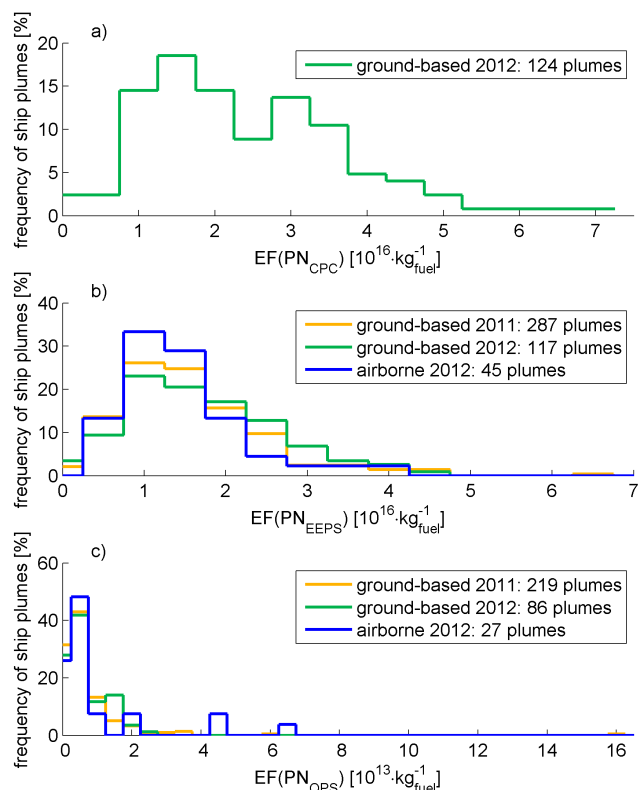
**Figure 8.** Frequency distribution of emission factors for particle number shown for **(a)** CPC ($>5\,\mu m$), **(b)** EEPS (5.6 to 560 nm) and **(c)** OPS (0.3 to 10 $\mu m$).



**Figure 9.** Frequency distribution of emission factors for particle mass. The data bases on the particle sizer measurements from the EEPS and the OPS. The size distribution of the OPS was truncated for size channels below 560 nm i.e., the upper size limit of the EEPS. Since no more data is available at this stage, the particles are assumed to be of spherical shape with a density of $1\,g\,cm^{-3}$.

tively. These ranges compare well with the results found in other studies (Petzold et al., 2008; Murphy et al., 2009; Jonsson et al., 2011; Lack et al., 2011; Alföldy et al., 2013; Beecken et al., 2014; Pirjola et al., 2014) between 0.3 and 2.55 particles $kg_{fuel}^{-1}$ or accordingly for particulate mass, between 0.4 and 3.77 $g_{PM}\,kg_{fuel}^{-1}$.

## 4.4 Comparison of modeled to measured data

The differences between measured and modeled emission factors by STEAM are summarized for each ship type in Fig. 10. The data for each ship was modeled considering the actual ship speed at the time of the plume measurement to estimate the engine load.

When comparing modeled and measured $SO_2$ emission factors, it can be seen that there is good agreement for passenger ships in international traffic and only a slight positive bias for the model for cargo and tanker ships. This hence indicates that the assigned model FSC for these ships is approximately correct. However, there are also many inland vessels for which there is a large positive bias in the model, indicating that the assigned model FSC of 1 % is much too high since the domestically running cargo and tanker ships actually had a measured FSC of around 0.4 % or less. This re-
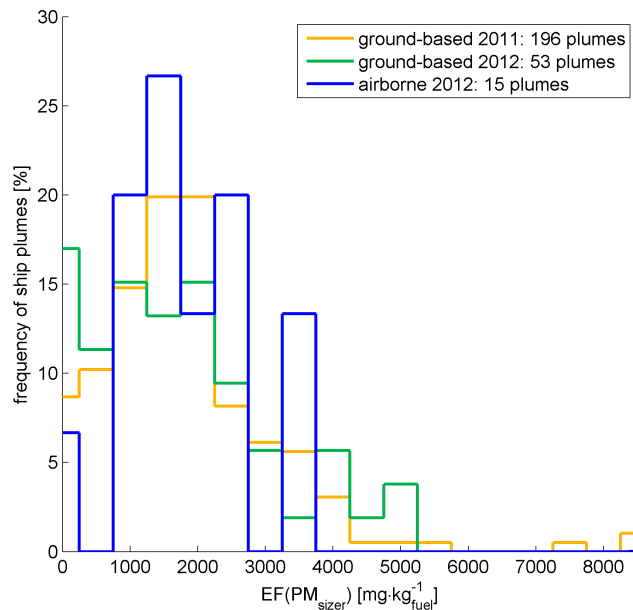
flects the restrictions of fuel used in inland waterway traffic, which to our knowledge prohibit the use of heavy fuel oil within the city borders due to ship-operation safety reasons. Improvements to the FSC predictions of especially inland vessels needs local knowledge and geographical restrictions. In future modeling work, the fuel assignment of inland waterway traffic must be considered in a more realistic manner because fuel type and sulfur content assignment will have an impact on both $SO_x$ and PM emission factors.

This fact was pointed out to the air quality authorities of the City of Saint Petersburg (Krylov et al., 2012), who assumed a FSC of 1 and 1.5 % for the primary fuel of 70 and 30 % of the ships, respectively, when carrying out air quality modeling. They later adapted the emission factors in their modeling to 0.17 and 1 %, based on the FSC data given in this paper with the consequence that shipping area had considerably less impact on air quality in the Saint Petersburg than originally estimated, especially for sulfur but also particles.

The modeled emission factors of $NO_x$ match well with the measurements for passenger ships and domestic tankers, as shown in Fig. 10. The average difference is around $3\,g_{NO_x}\,kg_{fuel}^{-1}$ (+4 % relative to average) and the spread for individual ships is in the order of the measurement uncertainty for $NO_x$. For domestic cargo ships, the average difference between the model and measurement results is $9\,g_{NO_x}\,kg_{fuel}^{-1}$ (−11 %) lower than the measured emissions.
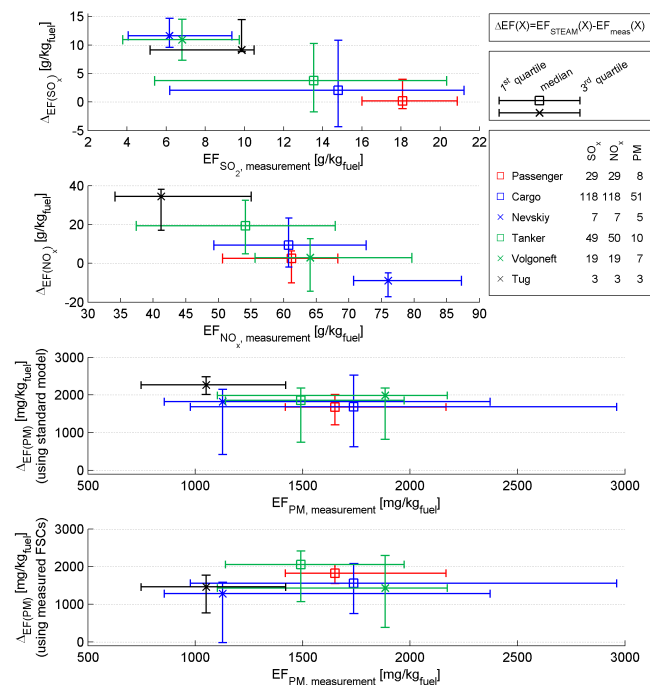
**Figure 10.** Comparison between modeled data by STEAM and measured data. The differences of the emission factors are shown group-wise for individual ships at same speed. Thus it is shown in the graphs by how much the STEAM model statistically exceeds the measured data. It should be considered that the modeled $SO_x$ was compared to the measured $SO_2$. Furthermore, the sum of the modeled emissions of organic carbon, elemental carbon, ash and $SO_4$ are compared to the measured size-distributed data between 5.6 nm and 10 μm under the assumption of a particle density of $1\,g\,cm^{-3}$, which were calculated using the FSCs originally assumed by the model and the FSCs obtained from the measurements. The number of the compared plumes for each type and species is presented by the number values in the legend.

Significant differences between the model and the measurement results can be seen for international running tankers (+40 %) and tug boats (+84 %). Even though only three tug boats were measured, they showed significantly lower $NO_x$ emissions than other ship types in the low-load conditions in the ship channel of Neva Bay.

The low values of measured $NO_x$ emission factors for certain, very new, vessels were observed already at IMO Tier 3 level. The measurements indicate that certain, recently built vessels already operate following the IMO tier 3 regulations. Other ships showing low $NO_x$ emissions are known to run with engines capable of using both gas and diesel. In the case of dual-fuel engines, low-load operation in STEAM leads to switch from gas mode to diesel mode. The speed limit of 10 kn is already low enough to trigger this behavior in the model and $NO_x$ emission factors defined by engine rpm and IMO $NO_x$ curve is then applied.

The modeling of particulate matter emissions is complex due to the uncertainties in assumptions about the FSC, engine load and the mass and composition of the emitted particles used. Large differences between modeled and measured emissions can be seen for particles in Fig. 10. The deviations found might be partly due to the assumed unity density (see for example Virtanen et al., 2002, Petzold et al., 2008, Murphy et al., 2009, Barone et al., 2011, Kuwata et al., 2012, and Pennington et al., 2013, for the typical range of densities), the limited size range for the measured data and assumptions made in STEAM. With respect to the latter, there are several uncertainty sources regarding the modeling of the particulate matter emissions.

First, the instantaneous main and auxiliary engine power level predictions will have an impact on modeled engine loads. Load levels of engines, in turn, will have an impact on calculated emission factors and instantaneous values of specific fuel consumption, thus changing the mass-based emission factors in the model. For the model, engine load and load balancing is more straightforward for a single two-stroke main engine than for a setup of several four-stroke main engines, in the case of which the number of active main engines may vary depending on variable power needs of the vessel. A comparison of the model and measured results for EF(PM) of ships using two-stroke engines did not show a significant improvement in this study. Unfortunately, the lack of observations from the ships' engine rooms regarding the operational state of the engines hinders a more detailed analysis. However, it is unlikely that these uncertainties are the single cause for the deviations between measured and modeled results of more than 100 %.

Second, the FSC will have a major impact on the modeled PM emission factor. In STEAM, the cheapest possible fuel (with higher sulfur content) is assigned to vessels, defined by geographical limitations (SECA/non-SECA, local legislation for port areas) and technical feasibility of using residual fuel. A recalculation with the model using FSC from the measurement of the individual ships as shown in the bottom plot in Fig. 10 did not lead to a major improvement.

Third, some differences between the modeled and measured results can be explained by unknown parameters for certain domestic ships, for which standard parameters for small vessels were used. Small vessels in domestic operations do not need to undergo the IMO registry procedure and the level of technical details of these vessels in STEAM database is low. For this reason, small vessels are assigned the generic tugboat type, which is bound to lead to inaccuracies in vessel performance and emissions calculations.

Fourth, the conditions of experimental measurements, on which STEAM emission factors for PM are based (see Jalkanen et al., 2012, for details), do not necessarily correspond to the measurement conditions used in the plume chasing approach used in the current work. The emission factors of fresh exhaust are quite different from those of the aged plume and sample analysis in laboratory conditions may have an

impact on PM mass determination when compared to in situ measurements. The aerosol chemistry after the emission of the plume is not trivial, and considering that the plumes are already aged by several minutes there are significant changes in number and mass of the emitted particles. Direct comparison of PM results from plume chasing studies with emission modeling would necessitate the use of PM emission factors which represent fresh exhaust, and consecutive modeling should be done using a plume model with a detailed description of aerosol processes. This was not done during the current work, however, and it requires further study. It may be necessary to develop separate ship emission modeling schemes for short-range studies (both in space and time) of aerosols and for regional scale modeling, unless regional transport models can include relevant aerosol physics modules describing gas/particle partitioning in a short timescale (Robinson et al., 2007; Tian et al., 2014).

It was clearly observed in the modeling results that the misallocation of FSC for ships, especially for domestic traffic using low sulfur fuel, will easily lead to SO$_x$ and PM emission factors of which the latter are over twice higher than what was measured in this work. However, the model does not allow for higher fuel sulfur content for vessels than what is allowed by current legislation unless the user assigns the fuel sulfur content manually. Currently, there is no centralized registry for the properties of fuel used in each vessel, making emission modeling challenging for SO$_x$ and PM. In this regard, the work reported improves the knowledge of the fuel sulfur content of Baltic Sea shipping.

## 5 Summary and conclusions

During two campaigns in summer 2011 and summer 2012, ship emissions in the Gulf of Finland, especially in the Neva Bay area, were measured from various platforms: boat, helicopter and from shore. Altogether 466 plumes of 311 individual vessels were sampled.

The sampled plumes showed a bi-modal distribution of the SO$_2$ emission factors. Ships in the lower mode emitted in average 4.6 $g_{SO_2}\,kg_{fuel}^{-1}$ and in the higher mode 18.2 $g_{SO_2}\,kg_{fuel}^{-1}$. It was observed that locally operating ships like the fast ferries, Nevsky cargo ships, Volgoneft tanker vessels and tugs generally emit less SO$_2$ than domestically operating passenger and cargo ships. Passenger ships appeared to be located significantly towards the upper end on the SO$_2$ emission factor scale and entirely running on fuel with higher sulfur contents, around 1 %. Measurements in 2011 showed compliance with the 1 % SECA sulfur limit in 90 % of the 255 observed plumes. In 2012, 97 % of the measurements of 211 plumes indicated compliance.

The distribution of the NO$_x$ emission factor indicated a mono-modal distribution around an average of 58 $g_{NO_x}\,kg_{fuel}^{-1}$. This average was found to be around 12 % below the values found in other studies, probably because of the low speed with low engine loads which impact the emissions rate.

The emission factor uncertainties of 21 % for SO$_2$ and around 25 % for NO$_x$ found are comparable to similar studies (Alföldy et al., 2013).

The particle measurements show that the main contribution to the particle number for particle sizes between 5.6 nm and 10 μm comes from particles below 65 nm. Around 70 % of the particle mass appears to be due to particles below 300 nm.

The conducted ground-based measurements provide a good overview about the distribution of all passing vessels and about the general distribution of emission factors at the measurement sites. Most ground-based measurements were conducted at the ship passage between St. Petersburg and Kronstadt. Many of the domestic and all of the international shipping vessels that travel between St. Petersburg and the Baltic pass this way. Furthermore, these measurements were conducted over several days, where both day and night traffic were observed.

The strength of the helicopter-based measurements was that a greater sea area could be covered and the emissions of more ships could be measured within a short time period. The ships could be arbitrarily selected and inspected. Further, it was possible to cross the same plume several times to decrease uncertainty.

The measured data was compared to modeled data using the STEAM model of the Finnish Meteorological Institute. The result indicated that the assumed FSC might be overestimated by the model for certain ship types, especially those engaging in domestic traffic. Overall, the NO$_x$ emissions compared well with the modeled results, while there is a significant difference concerning the particle emissions which is only partially due to uncertainties in fuel sulfur content assumptions made in STEAM and requires further evaluation.

## References

Agrawal, H., Malloy, Q. G. J., Welch, W. A., Wayne Miller, J., and Cocker, D. R.: In-use gaseous and particulate matter emissions from a modern ocean goingvessel, Atmos. Environ., 42, 5504–5510, doi:10.1016/j.atmosenv.2008.02.053, 2008.

Alföldy, B., Lööv, J. B., Lagler, F., Mellqvist, J., Berg, N., Beecken, J., Weststrate, H., Duyzer, J., Bencs, L., Horemans, B., Cavalli, F., Putaud, J.-P., Janssens-Maenhout, G., Csordás, A. P., Van Grieken, R., Borowiak, A., and Hjorth, J.: Measurements of air pollution emission factors for marine transportation in SECA, Atmos. Meas. Tech., 6, 1777–1791, doi:10.5194/amt-6-1777-2013, 2013.

AMSA (Australian Maritime Safety Authority): Protocol of 1997 to amend the International Convention for the Prevention of Pollution from Ships, 1973, as modified by the Protocol of 1978 relating thereto (MARPOL PROT 1997) Annex VI, available at: https://imo.amsa.gov.au/public/parties/marpol97prot.html (last access: 30 January 2015), 2014.

Balzani Lööv, J. M., Alfoldy, B., Gast, L. F. L., Hjorth, J., Lagler, F., Mellqvist, J., Beecken, J., Berg, N., Duyzer, J., Westrate, H., Swart, D. P. J., Berkhout, A. J. C., Jalkanen, J.-P., Prata, A. J., van der Hoff, G. R., and Borowiak, A.: Field test of available methods to measure remotely SOx and NOx emissions from ships, Atmos. Meas. Tech., 7, 2597–2613, doi:10.5194/amt-7-2597-2014, 2014.

Barone, T. L., Lall, A. A., Storey, J. M. E., Mulholland, G. W., Prikhodko, V. Y., Frankland, J. H., Parks, J. E., and Zachariah, M. R.: Size-resolved density measurements of particle emissions from an advanced combustion diesel engine: Effect of aggregate morphology, Energy and Fuels, 25, 1978–1988, 2011.

Beecken, J., Mellqvist, J., Salo, K., Ekholm, J., and Jalkanen, J.-P.: Airborne emission measurements of SO$_2$, NO$_x$ and particles from individual ships using a sniffer technique, Atmos. Meas. Tech., 7, 1957–1968, doi:10.5194/amt-7-1957-2014, 2014.

Borkowski, T., Kasyk, L., and Kowalak, P.: Assessment of ship's engine effective power, fuel consumption and emission using the vessel speed, Journal of KONES, 18, 31–39, 2011.

Cappa, C. D., Williams, E. J., Lack, D. A., Buffaloe, G. M., Coffman, D., Hayden, K. L., Herndon, S. C., Lerner, B. M., Li, S.-M., Massoli, P., McLaren, R., Nuaaman, I., Onasch, T. B., and Quinn, P. K.: A case study into the measurement of ship emissions from plume intercepts of the NOAA ship *Miller Freeman*, Atmos. Chem. Phys., 14, 1337–1352, doi:10.5194/acp-14-1337-2014, 2014.

Corbett, J. J., Fischbeck, P. S., and Pandis, S. N.: Global nitrogen and sulfur inventories for oceangoing ships, J. Geophys. Res.-Atmos., 104, 3457–3470, 1999.

Corbett, J. J., Winebrake, J. J., Green, E. H., Kasibhatla, P., Eyring, V., and Lauer, A.: Mortality from ship emissions: A global assessment, Environ. Sci. Technol., 41, 8512–8518, 2007.

Hallquist, Å. M., Fridell, E., Westerlund, J., and Hallquist, M.: On-board measurements of nanoparticles from a SCR-equipped marine diesel engine, Environ. Sci. Technol., 47, 773–780, 2013.

Hering, S. V., Stolzenburg, M. R., Quant, F. R., O'Berreit, D. R., and Keady, P. B.: A laminar-flow, water-based condensation particle counter (WCPC), Aerosol. Sci. Tech., 39, 659–672, 2005.

Hinds, W. C.: Aerosol technology : properties, behavior, and measurement of airborne particles, Wiley, New York, 1999.

IHS Global: IHS Maritime, Chemin de la Mairie, Perly, Geneva, Switzerland, 2014.

Jalkanen, J. P. and Johansson,L.: Emissions from Baltic Sea shipping in 2012, available at: http://www.helcom.fi/baltic-sea-trends/environment-fact-sheets/hazardous-substances/emissions-from-baltic-sea-shipping/ (last access: 28 August 2014), 2013.

Jalkanen, J.-P., Brink, A., Kalli, J., Pettersson, H., Kukkonen, J., and Stipa, T.: A modelling system for the exhaust emissions of marine traffic and its application in the Baltic Sea area, Atmos. Chem. Phys., 9, 9209–9223, doi:10.5194/acp-9-9209-2009, 2009.

Jalkanen, J.-P., Johansson, L., Kukkonen, J., Brink, A., Kalli, J., and Stipa, T.: Extension of an assessment model of ship traffic exhaust emissions for particulate matter and carbon monoxide, Atmos. Chem. Phys., 12, 2641–2659, doi:10.5194/acp-12-2641-2012, 2012.

Johnson, T., Caldow, R., Pöcher, A., Mirme, A., and Kittelson, D.: A new electrical mobility particle sizer spectrometer for engine exhaust particle measurements, SAE Technical Paper 2004-1-1341, 2004 SAE World Congress Detroit (MI), United States, 2004.

Jonsson, A. M., Westerlund, J., and Hallquist, M.: Size-resolved particle emission factors for individual ships, Geophys. Res. Lett., 38, L13809, doi:10.1029/2011GL047672, 2011.

Kley, D. and McFarland, M.: Chemiluminescence detector for NO and NO$_2$, Atmos. Technol., 12, 63–69, 1980.

Krylov, B. S., Novikov, L. A., and Frank-Kamenetsky, D. A.: Opredeleniye massy vrednykh (zagryaznyayushchikh) veshchestv, vybrasyvayemykh vodnym transportom v atmosferu Sankt-Peterburga [Determining the mass of harmful substances (pollutants) emitted into the atmosphere waterways of St. Petersburg], Okhrana atmosfernogo vozdukha, Atmosfera [Air Protection. Atmosphere], SRI Atmosphere, St. Petersburg, Russia, 1, 21, 2012.

Kuiken, K.: Diesel Engines for Ship Propulsion and Power Plants Vol 1, Target Global Energy Training, Onnen, the Netherlands, 2008.

Kuwata, M., Zorn, S. R., and Martin, S. T.: Using elemental ratios to predict the density of organic material composed of carbon, hydrogen, and oxygen, Environ. Sci. Technol., 46, 787–794, doi:10.1021/es202525q, 2012.

Lack, D. A., Cappa, C. D., Langridge, J., Bahreini, R., Buffaloe, G., Brock, C., Cerully, K., Coffman, D., Hayden, K., Holloway, J., Lerner, B., Massoli, P., Li, S. M., McLaren, R., Middlebrook, A. M., Moore, R., Nenes, A., Nuaaman, I., Onasch, T. B., Peischl, J., Perring, A., Quinn, P. K., Ryerson, T., Schwartz, J. P., Spackman, R., Wofsy, S. C., Worsnop, D., Xiang, B., and Williams, E.: Impact of fuel quality regulation and speed reductions on shipping emissions: implications for climate and air quality, Environ. Sci. Technol., 45, 9052–9060, doi:10.1021/es2013424, 2011.

Luke, W. T.: Evaluation of a commercial pulsed fluorescence detector for the measurement of low-level SO$_2$ concentrations during the gas-phase sulfur intercomparison experiment, J. Geophys. Res.-Atmos., 102, 16255–16265, 1997.

Mellqvist, J. and Berg, N.: Final Report to Vinnova: Identification of gross polluting ships, RG Report No. 4, ISSN 1653 333X, Chalmers University of Technology, Göteborg, Sweden, 2010.

Mellqvist, J., Beecken, J., Ekholm, J., and Salo, K.: Remote Compliance Monitoring of Gas Emissions from Shipping to Enforce International Policies, in preparation, 2015.

MEPC: Marine Environment Protection Committee, Interim Guidelines for Voluntary Ship $CO_2$ Emission Indexing for Use in Trials, IMO, London, United Kingdom, 2005.

MEPC: Marine Environment Protection Committee, Amendments to the technical code on control of emission of nitrogen oxides from marine diesel engines – $NO_x$ Technical Code, IMO, London, United Kingdom, 2008.

Moldanová, J., Fridell, E., Popovicheva, O., Demirdjian, B., Tishkova, V., Faccinetto, A., and Focsa, C.: Characterisation of particulate matter and gaseous emissions from a large ship diesel engine, Atmos. Environ., 43, 2632–2641, doi:10.1016/j.atmosenv.2009.02.008, 2009.

Moldanová, J., Fridell, E., Winnes, H., Holmin-Fridell, S., Boman, J., Jedynska, A., Tishkova, V., Demirdjian, B., Joulie, S., Bladt, H., Ivleva, N. P., and Niessner, R.: Physical and chemical characterisation of PM emissions from two ships operating in European Emission Control Areas, Atmos. Meas. Tech., 6, 3577–3596, doi:10.5194/amt-6-3577-2013, 2013.

Murphy, S., Agrawal, H., Sorooshian, A., Padró, L. T., Gates, H., Hersey, S., Welch, W. A., Jung, H., Miller, J. W., Cocker III, D. R., Nenes, A., Jonsson, H. H., Flagan, R. C., and Seinfeld, J. H.: Comprehensive simultaneous shipboard and airborne characterization of exhaust from a modern container ship at sea, Environ. Sci. Technol., 43, 4626–4640, 2009.

O'Keefe, A. and Deacon, D. A. G.: Cavity ring-down optical spectrometer for absorption measurements using pulsed laser sources, Rev. Sci. Instrum., 59, 2544–2551, 1988.

Pennington, M. R., Bzdek, B. R., DePalma, J. W., Smith, J. N., Kortelainen, A.-M., Hildebrandt Ruiz, L., Petäjä, T., Kulmala, M., Worsnop, D. R., and Johnston, M. V.: Identification and quantification of particle growth channels during new particle formation, Atmos. Chem. Phys., 13, 10215–10225, doi:10.5194/acp-13-10215-2013, 2013.

Petzold, A., Hasselbach, J., Lauer, P., Baumann, R., Franke, K., Gurk, C., Schlager, H., and Weingartner, E.: Experimental studies on particle emissions from cruising ship, their characteristic properties, transformation and atmospheric lifetime in the marine boundary layer, Atmos. Chem. Phys., 8, 2387–2403, doi:10.5194/acp-8-2387-2008, 2008.

Pirjola, L., Pajunoja, A., Walden, J., Jalkanen, J.-P., Rönkkö, T., Kousa, A., and Koskentalo, T.: Mobile measurements of ship emissions in two harbour areas in Finland, Atmos. Meas. Tech., 7, 149–161, doi:10.5194/amt-7-149-2014, 2014.

Robinson, A. L., Donahue, N. M., Shrivastava, M. K., Weitkamp, E. A., Sage, A. M., Grieshop, A. P., Lane, T. E., Pierce, J. R., and Pandis, S. N.: Rethinking organic aerosols: Semivolatile emissions and photochemical aging, Science, 315, 1259–1262, doi:10.1126/science.1133061, 2007.

Schlager, H., Baumann, R., Lichtenstern, M., Petzold, A., Arnold, F., Speidel, M., Gurk, C., and Fischer, H.: Aircraft-based Trace Gas Measurements in a Primary European Ship Corridor, TAC-Conference, Oxford, UK, 26–29 June 2006, 83–88, 2006.

Starcrest: Starcrest Consulting Group LLC, Port of Long Angeles: Inventory Air Emissions – 2011, Long Beach (CA), USA, 2012.

Tian, J., Riemer, N., West, M., Pfaffenberger, L., Schlager, H., and Petzold, A.: Modeling the evolution of aerosol particles in a ship plume using PartMC-MOSAIC, Atmos. Chem. Phys., 14, 5327–5347, doi:10.5194/acp-14-5327-2014, 2014.

UNCTAD: Review of Maritime Transport 2012, United Nations Publication, ISSN 0566-7682, ISBN: 978-92-1-112860-4, e-ISBN: 978-92-1-055950-8, 2013.

Virtanen, A., Ristimäki, J., Marjamäki, M., Vaaraslahti, K., Keskinen, J., and Lappi, M.: Effective density of diesel exhaust particles as a function of size, SAE Technical Paper 2002-01-0056, 2002 SAE World Congress Detroit (MI), United States, 2002.

Williams, E. J., Lerner, B. M., Murphy, P. C., Herndon, S. C., and Zahniser, M. S.: Emissions of $NO_x$, $SO_2$, CO, and HCHO from commercial marine shipping during Texas Air Quality Study (TexAQS) 2006, J. Geophys. Res.-Atmos., 114, D21306, doi:10.1029/2009JD012094, 2009.